X-ray Tomography of Short Fatigue Cracks in Ductile Iron

T.J. Marrow[1], H. Çetinel[2], S. MacDonald[1], P.J. Withers[1], A. Venslovas[3], and M. Leonaviçius[3]

[1] Manchester Materials Science Centre, UMIST, P.O. Box 88, Manchester, M60 1QD, UK.
[2] Dokuz Eylül University, Faculty of Engineering, Department of Metallurgical and Materials Engineering, Bornova, 35100, İzmir, Turkey.
[3] Gedeminas Vilnius Technical University, Vilnius, Lithuania.

ABSTRACT: *X-ray tomography, using the 2 μm high resolution ESRF synchrotron facility (Grenoble) has been used to study the three-dimensional shape of a short fatigue crack in a ferrite/pearlite cast iron. The technique allows visualisation of the defect and rapid characterisation of the distribution of defects, which would normally require time-consuming serial sectioning.*

This paper discusses the technique of X-ray tomography and its application to short crack fracture mechanics and failure research.

INTRODUCTION

Computed X-ray tomography is a non-destructive technique that allows the construction of three-dimensional images of defects within materials [1-3]. Fatigue crack nuclei in a ferrite-pearlite ductile cast iron were examined using X-ray tomography. The aim of the experiment was to demonstrate the use of high-resolution tomography as a tool for observation of 3-dimensional crack shape. This technique had previously been applied to crack nuclei in an austempered ductile cast iron [4].

EXPERIMENT AND RESULTS

A low alloy ferrite-pearlite ductile cast iron was obtained as a plate (thickness 20 mm) that had been cut from a large casting. The microstructure had shrinkage pores up to several hundred microns in size. The rectangular specimen blanks, measuring approximately 250 mm x 26

mm x 11.5 mm, were prepared to a metallographic finish with 0.25 μm diamond polishing medium. The specimen was tested in four-point bending at a frequency of 12 Hz. The fatigue test was at a stress amplitude of 200 MPa, about a mean stress of 244 MPa. The ratio of minimum to maximum stress (R-ratio) was 0.1. Acetate replicas were taken at intervals during the test to record the development of fatigue cracks. The replicated area measured approximately 20 mm x 80 mm.

The test failed after approximately 800,000 cycles by the unstable propagation of a single large crack. Several cracks larger than a few mm were also observed as well as many smaller cracks. All the larger cracks were found to nucleate at pores (Figure 1). Smaller cracks were observed to nucleate at graphite nodules. These were often arrested at ferrite/pearlite or ferrite/ferrite grain boundaries (Figure 2).

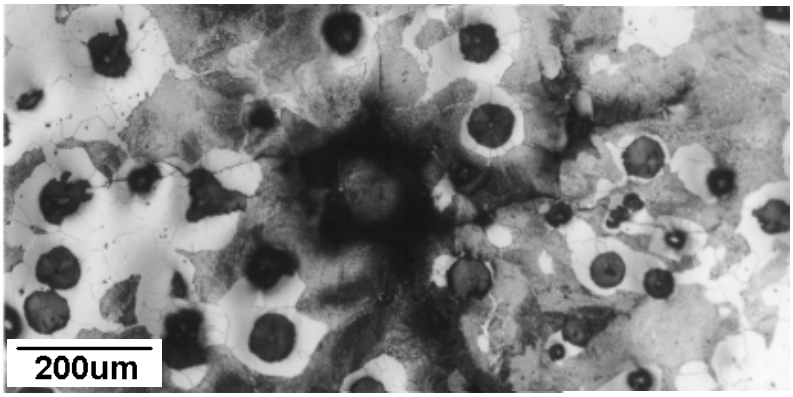

Figure 1: Fatigue crack (crack L in Figure 3) in ferrite/pearlite ductile iron, nucleated at a pore. The specimen was tested above the fatigue limit. The tensile axis was vertical.

The lengths of twelve cracks nucleated from pores were measured in successive replicas to determine the crack growth rate as a function of crack length. The total surface crack length was recorded, including the length of the pore in the crack plane (Figure 3). The crack growth rate data is compared with the predicted growth rate for long cracks in a similar ductile cast iron [5] calculated for a semi-circular surface crack under the same stress amplitude and R-ratio. The long crack fatigue behaviour has previously been found to be insensitive to microstructure [6] above the threshold, although crack closure effects can influence the threshold [5]. A

long crack threshold value of 5.7 MPa√m was assumed for a ferrite-pearlite cast iron at an R-ratio of 0.15 [5].

Crack decelerations and accelerations were observed, with a tendency for the short crack growth rate to increase with increasing crack length. Short crack propagation was also observed below the long crack threshold. This behaviour is typical of short fatigue cracks, which are sensitive to the microstructure [7,8]. With increasing crack length, the highest short crack growth rates were comparable to the prediction for semi-circular surface flaws from long crack data, although the average velocity of growth tended to be less than predicted. The microstructure at the position of significant decelerations of crack velocity was examined. The decelerations were found to occur at microstructure boundaries. For example, a significant deceleration occurred for crack L (Figure 3) where the crack propagated from pearlite to ferrite (Figure 4). Significant retardations and crack arrests (i.e. a growth rate of less than 10^{-5} μm/cycle) were also observed at pearlite/pearlite and ferrite/pearlite interfaces.

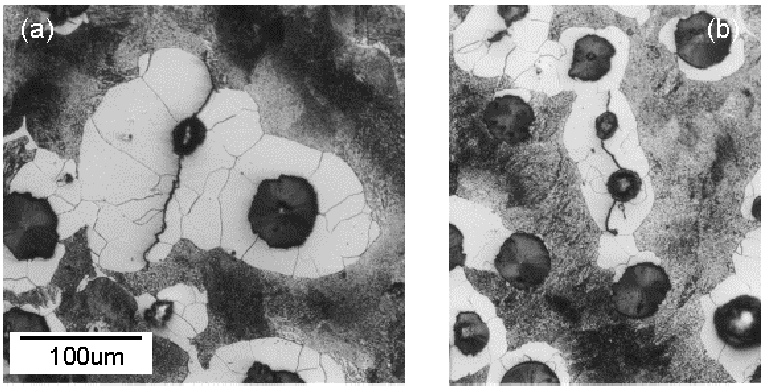

Figure 2: Stable fatigue crack nuclei. The tensile axis was horizontal.

Microtomographic x-ray analysis was performed at the European Synchrotron Radiation Facility (ESRF) using the high-resolution tomographic beam-line (ID19). The electron beam energy was 6 GeV and the white beam was restricted by slits and monochromated by a set of two parallel silicon single crystals to select photons of energy 32 keV. The large distance of about 140 m between the source and the experimental hutch on ID19, together with a small x-ray source size (50-100 μm), leads to a high lateral coherence of the photons. The distance between the sample and detector, which is a CCD camera developed at the ESRF, was set to about

120 mm. This setup combined with the high lateral coherence has been shown [3] to lead to an improvement in the detection of phase features like cracks due to 'phase contrast' which superimposes onto the regular attenuation contrast. In collecting the data, the sample was rotated in the beam to provide a set of 900 radiographs (one radiograph every 0.2°), which were then used by reconstruction software to give a 3D numerical image of the studied material. The resolution was approximately 2 μm.

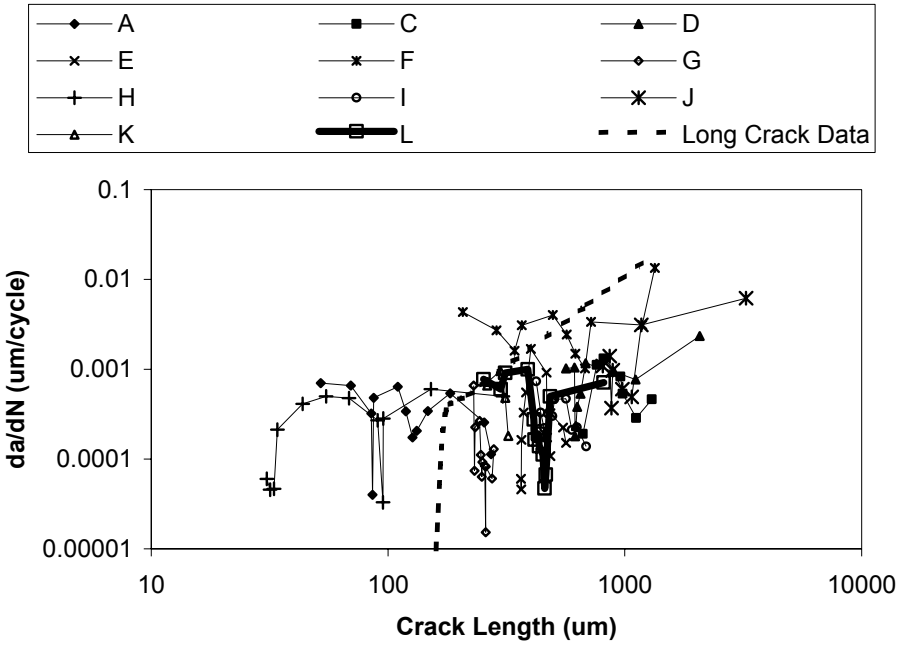

Figure 3: Variation of crack growth rate with crack length for short cracks in ductile cast iron, compared with long crack behaviour [5] calculated for a semi-circular surface flaw.

Due to limited time on the facility, only one crack could be examined using high resolution X-ray tomography. Crack L (Figure 1) was a crack approximately 0.8 mm in length. The sample was cut from the tensile surface using a diamond saw and ground to size leaving the tensile surface undamaged. The sample length was approximately 10 mm parallel to the tensile stress axis, with a width of 1 mm. The sample thickness was approximately 0.5 mm.

Tomographic images of the crack are shown in Figure 5 and Figure 6. The matrix has been rendered transparent in Figure 5 and opaque in Figure 6 to assist with visualisation of the crack shape. The crack is not semi-circular, but has the form of a pair of lobes initiated at the pore. The complex crack shape (Figure 6) implies that the crack nuclei initiated at several points around the pore, coalescing to develop the observed crack.

DISCUSSION

These observations confirm that crack nuclei in ferrite/pearlite ductile cast iron interact with the microstructure as they propagate from the nucleating defect. The most significant flaws were shrinkage pores. The cracks decelerate, and may arrest, as they encounter boundaries in the microstructure, which may be grain boundaries or phase boundaries. The grain and phase boundaries are assumed to affect crack growth due to blockage of slip and the requirement to re-initiate crack growth. The microstructure can therefore affect the fatigue limit, and the fatigue life above the fatigue limit.

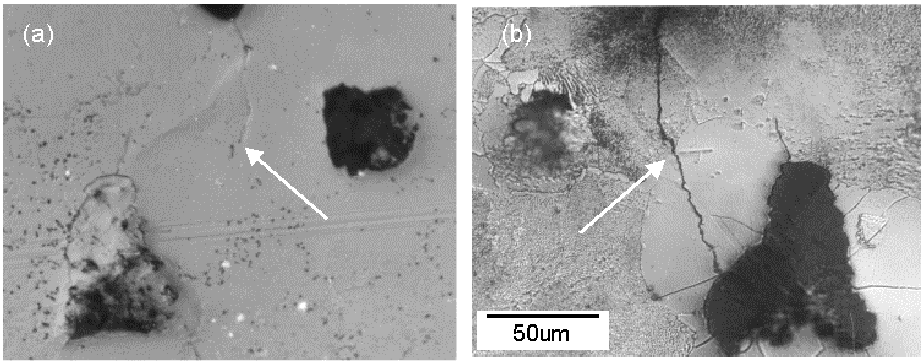

Figure 4: Crack retardation at pearlite/ferrite interface in crack L (Figure 3). The crack propagated from top to bottom of the image. (a) Replica showing crack tip location at lowest growth rate (marked with arrow). (b) Optical micrograph of specimen showing corresponding location (marked with arrow).

The fatigue limit in ductile irons is affected by the graphite nodule size, shape and distribution [9-11], and is sensitive to the matrix microstructure. The fatigue limit in ductile irons with a ferrite/pearlite matrix has been found to be affected by the continuity of the ferrite; a higher fatigue limit is

measured when the ferrite is non-continuous [10]. The observation of crack/microstructure interactions (Figure 4) implies that the phase boundaries in the discontinuous ferrite/pearlite microstructure increase the fatigue endurance limit by retarding the propagation of the fatigue crack nucleus.

The tomographic technique has limited resolution of tightly closed cracks. The small crack nucleated at the nearly graphite nodule that is visible in the replica and optical section (Figure 4) is not observed by tomography, although the more open dominant crack nucleus is clearly observed (Figure 6). The resolution of the crack may be improved by making observations while the specimen is under load. Higher resolution can be achieved using improved optics, but this restricts the specimen size.

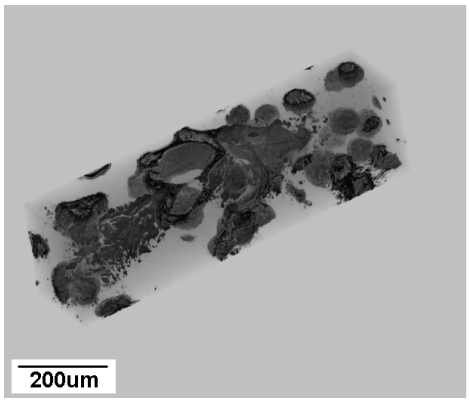

Figure 5: Tomographic image of crack L. This fatigue crack (crack L in Figure 3) was nucleated at a pore in a ferrite-pearlite ductile cast iron. The same crack is shown in Figure 1.

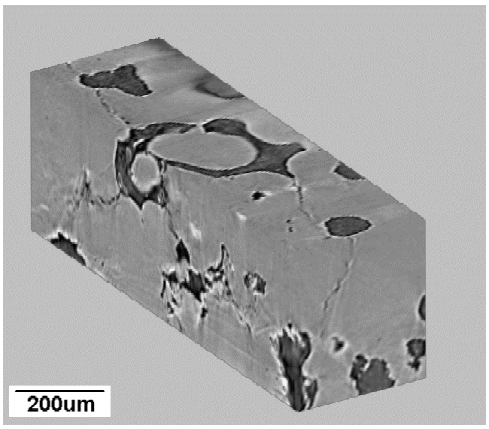

Figure 6: Tomographic image of crack L (Figure 5). The matrix has been rendered opaque to illustrate the complex crack shape.

Engineering fracture mechanics aims to model the connection between the fatigue life and casting defects, such as porosity and inclusions [12-16]. However, the models are over-conservative for small defects, typically less than 200 μm in size, such as micro-porosity. This is principally because they do not take account of the interaction between the defect size and shape and the heterogeneity of the microstructure on the same size scale. Small defects are becoming more significant as improved production methods and quality control eliminate the larger defects in castings. It is therefore necessary to develop fracture mechanics models applicable to small defects and long lifetimes. Consequently, damage tolerant design of castings

requires an understanding of short cracks and microstructure fracture mechanics. Modelling the fatigue lifetime of components above the fatigue limit requires knowledge of the development of the three-dimensional crack shape. Interactions between adjacent small defects, such as crack coalescence may either accelerate failure or lead to less damaging shallow defects. Previous studies of short crack behaviour have been restricted to two-dimensional observation of the crack length at the free surface. This provides no information about the development of the crack shape.

Conventional microscopy techniques only provide information of the crack length at a surface, whereas reconstruction from serial sectioning to determine the depth and shape of cracks [17] is slow and difficult. The tomographic analysis provides useful and easily visualised data about the size and shape of three-dimensional defects. These preliminary observations demonstrate that the assumption of a semi-circular flaw for the modelling of short crack growth can be inappropriate for short cracks in ferrite-pearlite cast irons. This shape may only develop for larger cracks following the coalescence of smaller cracks nucleated at pores. Short cracks may be less deep than suggested by their surface length, and consequently propagate more slowly than predicted (Figure 3). Work is now in progress to make in-situ tomography observations of short crack nucleation, propagation and coalescence in a ductile cast iron.

CONCLUSION

- Short fatigue crack nuclei in a ferrite-pearlite ductile cast iron are retarded and arrested by interaction with microstructure barriers.
- High resolution X-ray tomography has been demonstrated as a technique that can observe the three-dimensional shape of short fatigue cracks.

ACKNOWLEDGEMENTS

TJM gratefully acknowledges the financial support of the Royal Society and the Lithuanian Academy of Science, for the visit to the Gedeminas Technical University, Vilnius. We also acknowledge the financial support for study visits to Manchester for HÇ from the British Council, TÜBİTAK (The Scientific and Technical Research Council of Turkey) and Dokuz Eylül University. We are very grateful to Dr P. Cloetens (ESRF, Grenoble)

and Prof. J-Y Buffière (Lyons) for their assistance with the X-ray microtomography.

REFERENCES

1. P.M. Mummery, B. Derby, P. Anderson, G.R. Davis and J.C. Elliott (1995). *J. Microscopy*, **177**, 399-406.
2. S. Savelli, J.-Y. Buffière and R. Fougères (2000). *Mater. Sci. Forum.* **331-337**, 197-202.
3. J.-Y. Buffière, E. Maire, P. Clotens, G. Lormand and R. Fougères (1999). *Acta Mater.* **47**, 1613-1625.
4. T.J. Marrow, H. Çetinel, M. Al-Zalmah, S. MacDonald, P.J. Withers and J. Walton (2002). *Fatigue Fract. Engng Mater. Struct.* **25**, *in press.*
5. D.J. Bulloch and J.H. Bulloch (1989). *Int. J. Pres. Ves. & Piping*, **36**, 289-314.
6. J. Pokluda and J. Švejcar (1999). *Fatigue 99*, Vol 1, 487-492, pub. HEP.
7. K.J. Miller (1987). *Fatigue Frac. Engng. Mater. Struct.*, 1987, **10**, 95-113.
8. K.J. Miller (1993). *Mater. Sci. Tech.*, **9**, 453-462.
9. M. Sofue, S. Okada and T. Sasaki (1978). *AFS Transactions*, **86**, 173.
10. D. Venugopalan, K.L. Pilon and A. Alagarsamy (1980). *AFS Transactions,* **88**, 697.
11. J.F. Janowak, A. Alagarsamy and D. Venugopalan (1982). *AFS Transactions*, **90**, 511.
12. S. Beretta, A. Blarasin, M. Endo, T. Giunti and Y. Murakami (1997). *Int. J. Fatigue* **19**, 319-333.
13. Y. Nadot, J. Mendez, N. Ranganathan and A.S. Beranger (1999). *Fatigue Fract. Engng Mater. Struct.* **22**, 289-300.
14. S. Beretta and Y. Muakami (1998). *Fatigue Fract. Engng Mater. Struc.* **21**, 1049-1065.
15. J.-Y. Buffière S. Savelli, P.H. Jouneau, E. Maire and R. Fougères (2001). *Mater. Sci. Engng* **A316**, 115-126.
16. P.J. Laz and B.M. Hillberry (1998). *Int. J. Fatigue* **20**, 263-270.
17. P. Clement, J.P. Angelli and A. Pineau (1984). *Fatigue Fract. Engng Mater. Struct.* **7**, 251-265.